ACS OMEGA

Open Access

This article is licensed under CC-BY-NC-ND 4.0

http://pubs.acs.org/journal/acsodf

Article

First-Principles Study on the Selective Separation of Toxic Gases by Mg-MOF-74

Dipak Adhikari,* Ravi Karki, Kapil Adhikari, and Nurapati Pantha

Cite This: *ACS Omega* 2024, 9, 4849−4856

Read Online

ACCESS | Metrics & More | Article Recommendations | Supporting Information

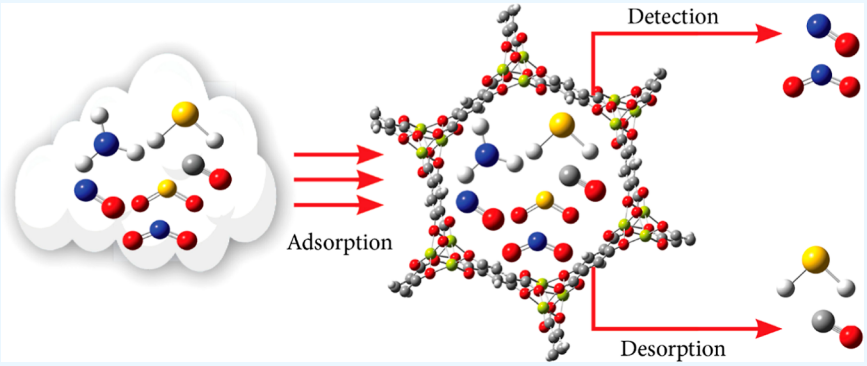

ABSTRACT: This study primarily focused on the detection and separation of toxic gases such as CO, H_2S, SO_2, NH_3, NO, and NO_2 by Mg-MOF-74, as well as assessing the stability of those toxic gases on it. The calculations were performed by using density functional theory as implemented in the Gaussian-09 and Quantum ESPRESSO suites of the program. GGA-type PBE-D2 functionals with a plane wave basis set were used in the optimization of the Mg-MOF-74 crystal, and hybrid-type B3LYP and M06 functionals with the 6-31G*basis set were used in cluster calculation. The binding energies of CO and H_2S with MOF were found to be in the physisorption range, whereas the energies of SO_2, NH_3, NO, and NO_2 were found to be in the chemisorption range. Based on binding energy, hardness, and softness studies, it was found that NO and NO_2 molecules were more stable in Mg-MOF-74, suggesting that Mg-MOF-74 is a good detector for NO and NO_2 molecules.

INTRODUCTION

Environmental pollution is one of the most problematic issues of our time, which not only contributes to climate change but also harms public and individual health.[1] The major pollutants are carbon monoxide, sulfur dioxide, hydrogen sulfide, nitrous oxide, ammonia, and other toxic gases.[2−4] Our health, the quality of our lives, and our longevity are all severely impacted by it. Additionally, it causes significant environmental problems, including ozone depletion, acid rain, agriculture, forest damage, and global climate change.[5] There are two ways to deal with this issue: either by lessening the emissions of pollutants into the environment or by capturing them from the atmosphere. Adsorbing these pollutants onto a suitable substance can address the problem. Therefore, our objective is to identify efficient adsorbents.

Metal−organic frameworks (MOFs) are architecturally constructed hybrid crystalline porous materials with metal-containing nodes connected by organic linkers. The size and shape of the pores depend on how many ligands are linked to the metal nodes. A longer organic linker offers more storage space, which, in turn, increases the surface area. Adding functional groups to the linkers makes it possible to change the MOFs' characteristics. There are practically endless combinations that can be made with metal ions and organic linkers. As a result, a wide range of these porous materials can be synthesized according to what we are looking for. As an emerging new class of porous solids, MOFs are expected to be extremely promising porous materials in various applications, including gas adsorption, separation,[6,7] catalysis,[8] sensing,[9] drug delivery,[10] etc. These materials have great potential for these applications because of their high porosity,[11] large surface area,[9] and structural tenability.[12]

The M-MOF-74 family (M = metal), also known as CPO-27-M or M_2(dobdc), is one of the promising MOF families that has been synthesized and thoroughly explored both computationally and experimentally. These are isostructural microporous MOFs with regular hexagonal pores. Open metal sites at the pore surface enhance their beauty. Mg-MOF-74 is a

Received: October 25, 2023
Revised: December 28, 2023
Accepted: January 9, 2024
Published: January 18, 2024

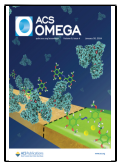

ACS Publications

© 2024 The Authors. Published by American Chemical Society

https://doi.org/10.1021/acsomega.3c08358
ACS Omega 2024, 9, 4849−4856

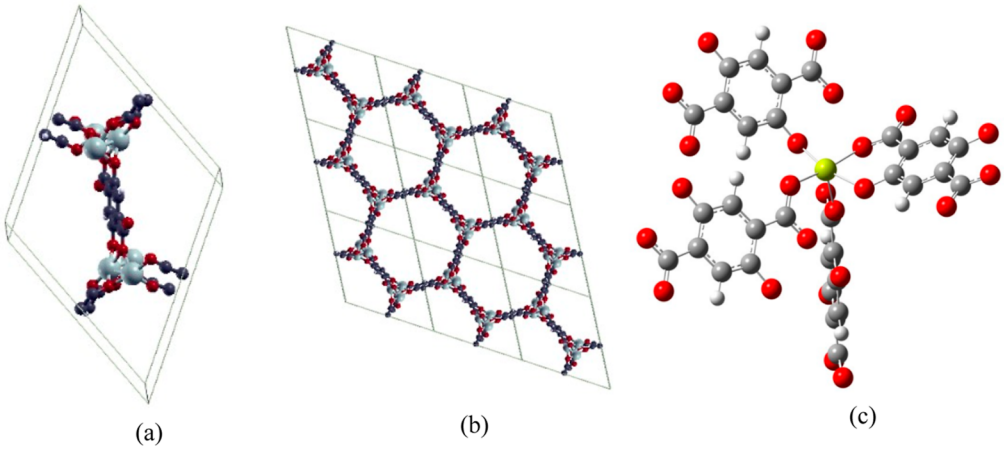

Figure 1. (a) Relaxed Structure of the Mg-MOF-74 crystal, (b) supercell structure of the Mg-MOF-74 crystal, and (c) cluster of Mg-MOF-74.

member of this family. The 2,5-dioxido-1,4-benzene-dicarboxylate ($dobdc^{4-}$) linkers that make up this MOF have huge one-dimensional pores with a diameter of around 12 Å, which are connected by helical chains of Mg^{2+} at their intersections.[13]

This study calculates the binding energies of six toxic gas molecules (CO, H_2S, SO_2, NH_3, and NO and NO_2) with Mg-MOF-74. In addition to calculating and analyzing the charge distribution on the MOFs, the highest occupied molecular orbital (HOMO) and lowest-lying unoccupied molecular orbital (LUMO) energies, HOMO−LUMO gap, hardness, and softness of the loaded and bare MOFs are also examined. The cluster and periodic models are both employed in the calculation. The structural and electrical properties of the Mg-MOF-74 crystal are determined using the periodic model. However, the binding energies, HOMO−LUMO gap, hardness, and softness are determined through the cluster model.

METHODOLOGY

The calculations were carried out by using density functional theory as implemented in the Quantum ESPRESSO[14] and Gaussian-09[15] suites of programs. Most of the calculations were based on the molecular cluster model. The major objective of employing molecular cluster models is to decrease computing expenses. Moreover, calculations on periodic systems using hybrid density functionals might not be feasible. Quantum ESPRESSO was used in the periodic model, while Gaussian-09 was used in the molecular cluster model. Starting from a triclinic primitive unit cell with 54 atoms, including six metal centers, a fully relaxed structure of Mg-MOF-74 was constructed. A GGA-type PBE-D2 functional with a plane wave basis set and an ultrasoft pseudopotential was used during the relaxation. Both the lattice vector and the atomic positions are simultaneously optimized until residual forces are smaller than 10^{-4} Ry/Bohrs and the stress tensor components are smaller than 0.1 kbar. A supercell of Mg-MOF-74 was created from its relaxed structure, and a cluster of the MOF was extracted from it. In cluster calculation, hybrid types B3LYP[16−18] and M06[19] functional with a 6-31G*[20,21] basis set were used. The relaxed structure, supercell structure, and cluster model of Mg-MOF-74 are shown in Figure 1.

The calculations were done under different spin states (multiplicity M = 1 and 3 for CO, H_2S, SO_2, and NH_3 and multiplicity M = 2 and 4 for NO and NO_2), and all the structures under study are found to be nonmagnetic, i.e., the lowest energies are obtained for the lowest multiplicities.

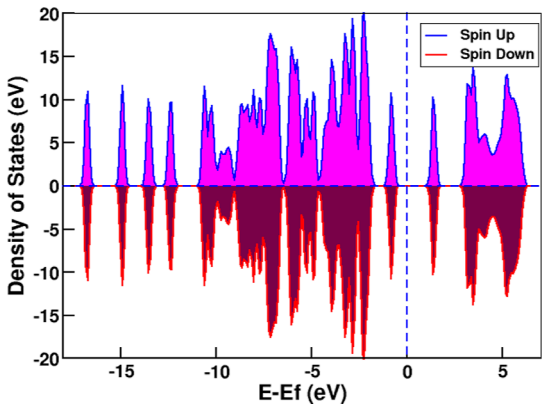

Figure 2. Density of states of the Mg-MOF-74 crystal.

Table 1. Binding Energy (kJ/mol) of Different Gas Molecules on Mg-MOF-74

molecules	method			
	B3LYP		M06	
	orientation of molecule		orientation of molecule	
CO[a]	C-head on	O-head on	C-head on	O-head on
	30.85	21.08	48.68	38.89
H_2S	V-up	V-down	V-up	V-down
	32.36	32.39	60.79	58.58
SO_2[b]	V-up	V-down	V-up	V-down
	50.73	52.22	80.02	81.28
NH_3	H-head on	N-head on	H-head on	N-head on
	119.36	119.36	138.24	139.56
NO	N-head on	O-head on	N-head on	O-head on
	479.03	448.36	546.34	539.20
NO_2	V-up	V-down	V-up	V-down
	455.80	473.71	521.26	531.90

[a]29 kJ/mol at 298 K.[25] [b]78.9 kJ/mol.[13]

The binding energies of gas molecules on MOF were calculated as

$$\Delta E = E_{mol} + E_{MOF} - E_{mol+MOF} \quad (1)$$

where E_{mol}, E_{MOF}, and $E_{mol+MOF}$ are the energy of the guest molecule, the energy of the bare MOF, and the energy of the loaded MOF.

The hardness and softness of the cluster were calculated as

https://doi.org/10.1021/acsomega.3c08358
ACS Omega 2024, 9, 4849−4856

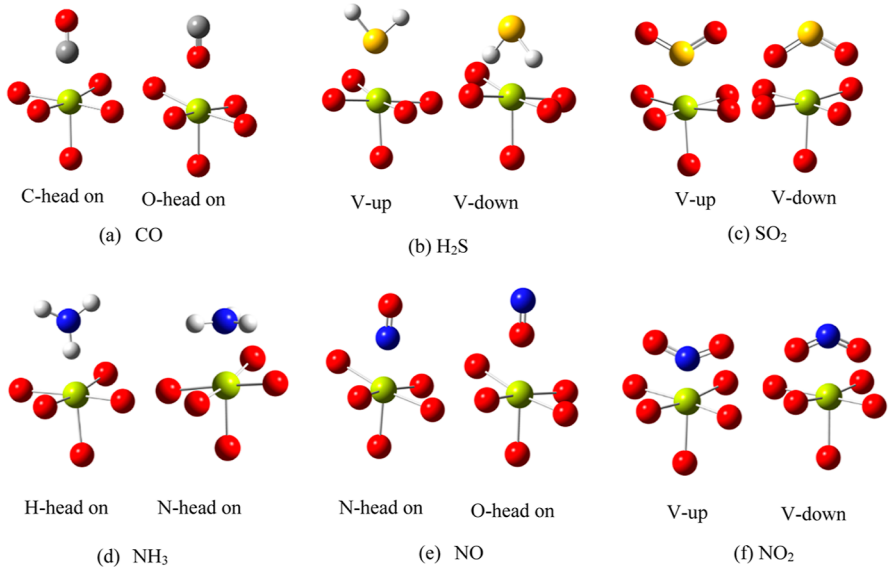

Figure 3. Orientation of different gas molecules on MOF.

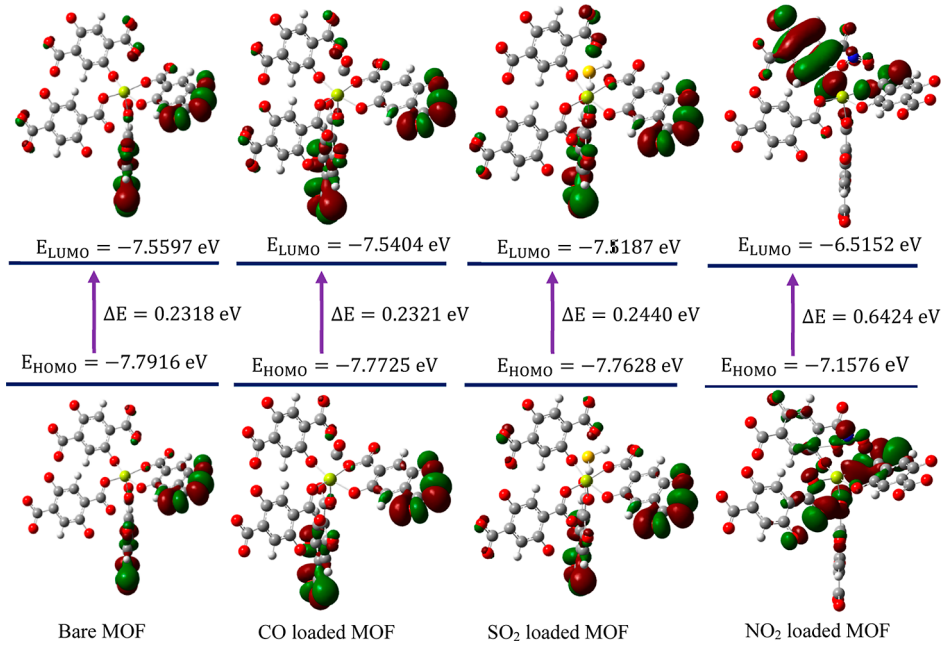

Figure 4. Molecular orbital distribution of bare and loaded Mg-MOF-74 in the B3LYP method.

Table 2. Chemical Reactivity Descriptors Using the B3LYP Method

parameters	bare MOF	CO-loaded MOF	H_2S-loaded MOF	SO_2-loaded MOF	NH_3-loaded MOF	NO-loadedMOF	NO_2-loaded MOF
E_{HOMO} (eV)	−7.79	−7.77	−7.74	−7.76	−7.72	−7.15	−7.16
E_{LUMO} (eV)	−7.56	−7.54	−7.49	−7.52	−7.47	−6.53	−6.52
ΔE (eV)	0.23	0.23	0.24	0.24	0.24	0.62	0.64
hardness η (eV)	0.12	0.12	0.12	0.12	0.12	0.31	0.32
softness S (eV)	4.31	4.31	4.09	4.10	4.08	1.59	1.56

$$\text{hardness, } \eta = \frac{E_{LUMO} - E_{HOMO}}{2} \quad (2)$$

$$\text{and softness, } S = \frac{1}{2\eta} \quad (3)$$

RESULT AND DISCUSSION

Structural and Electronic Properties of Mg-MOF-74. The crystallographic information provided by Rosen et al.[22] yielded the Mg-MOF-74 triclinic primitive unit cell, which consists of 54 atoms, including six magnesium centers. The optimized parameters of the Mg-MOF-74 crystal are found to be a = 6.80, b = 15.82, and c = 15.06 Å, respectively. The bond

https://doi.org/10.1021/acsomega.3c08358
ACS Omega 2024, 9, 4849−4856

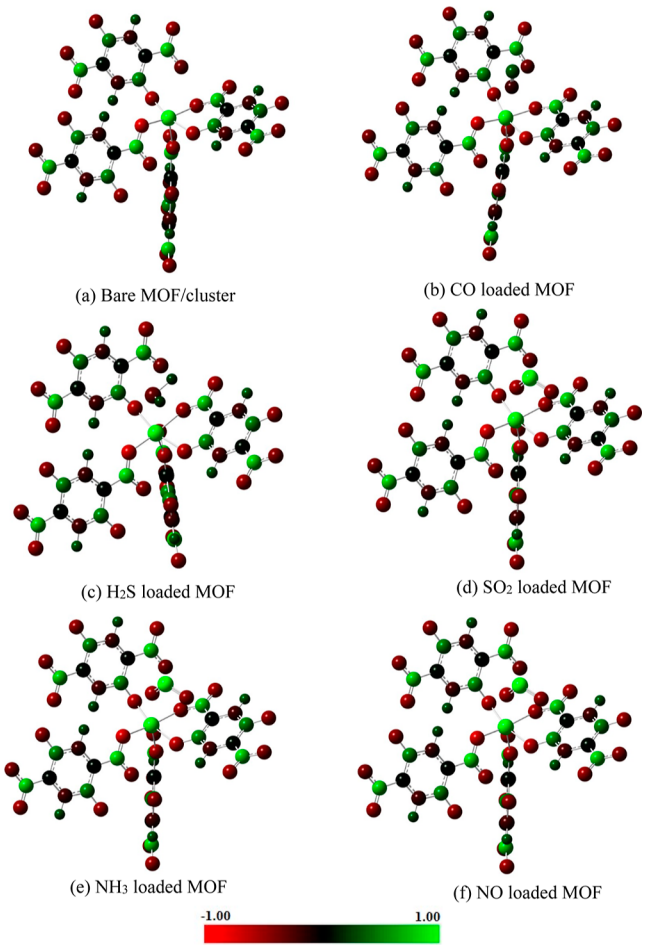

Figure 5. Charge distributions on MOF with various molecules.

Table 3. Total Charge on Guest Molecules after Adsorption

molecules	method	
	B3LYP	M06
CO	+0.083 (O-head on)	+0.086 (O-head on)
H_2S	+0.056 (V-down)	+0.064 (V-down)
SO_2	+0.07 (V-down)	+0.10 (V-down)
NH_3	+0.13 (N-head on)	+0.11 (N-head on)
NO	+0.07 (N-head on)	+0.09 (N-head on)
NO_2	−0.07 (V-down)	+0.01 (V-down)

length between magnesium cations and oxygen atoms in equatorial and axial positions is found to be 2.03 and 2.02 Å, which are almost identical to the experimental value.[23] Likewise, the density and volume of the crystal are found to be 0.91 g cm^{-3} and 1326.10 $Å^3$, respectively.

The density of states of the Mg-MOF-74 crystal is shown in Figure 2. This shows that the density of states is symmetrical for spin-up and spin-down electrons, showing that the material is nonmagnetic. The band gap of the crystal is found to be 1.20 eV, suggesting that it is semiconducting.

Binding Energy of Gas Molecules. The binding energies of six distinct gas molecules on Mg-MOF-74 are calculated by using two methods, B3LYP and M06, at the 6-31G* level theories, which are shown in Table 1. All the possible orientations are considered. For example: In the case of CO, O-head on, C-head on, and bridge orientations are considered. However, the bridge position is not preferred by the system and gets flipped/rotated in either the O-head on or the C-head on position. So only two orientations are chosen. Similarly, for other molecules, we checked all possible orientations. The orientations of different gas molecules on the MOF are shown in Figure 3. The binding energies of CO and H_2S are found within the range of physisorption. However, the binding energies of NO, NO_2, SO_2, and NH_3 are found within the range of chemisorption (>80 kJ/mol[24]). Therefore, NO, NO_2, SO_2, and NH_3 molecules cannot be desorbed from the MOF, but the CO and H_2S molecules can easily do so. The binding energies for CO and SO_2 are reported in the literature to be 29 kJ/mol at 298 K and 78.9 kJ/mol (DFT study), respectively, which support our results. Moreover, the binding energies of NO and NO_2 are significantly higher than those of other molecules, suggesting that these molecules are more stable in Mg-MOF-74.

Frontier Molecular Orbitals, Stability, and Detection of Gas Molecules. The HOMOs and the LUMOs are named Frontier molecular orbitals (FMOs). As they lie at the outermost boundaries of the electrons of the molecules, they are called FMOs. The molecular orbital distribution of Mg-MOF-74 after the adsorption of gas molecules is shown in Figure 4. Each of the HOMO and LUMO species has its own distinct energy. The best electron donor has the highest HOMO energy, whereas the best electron acceptor has the lowest LUMO energy. HOMO and LUMO both contain two colors, green and red. Green is used as a symbol for the positive phase, whereas red is used to symbolize the negative phase. The frontier orbital gap is crucial in determining the chemical stability of molecules. A molecule with a small frontier orbital gap is also known as a soft molecule since it is typically linked to higher chemical reactivity, more polarizability, and lower kinetic stability. Likewise, hard species are distinguished by wide frontier orbital gaps, which make them more stable and less reactive.

Table 2 lists the frontier orbital gap (HOMO−LUMO gap), hardness, and softness of the bare and loaded MOFs in the B3LYP methods. The reactivity descriptors, such as hardness (η) and softness (S), computed from the HOMO−LUMO gap, provide a clearer explanation of the stability of gas molecules on MOFs. As the value of hardness rises or the value of softness falls, the stability of the molecules increases. According to the B3LYP method, the hardness of bare MOF is 0.12 eV. The hardness of CO-loaded MOF, H_2S-loaded MOF, SO_2-loaded MOF, and NH_3-laded MOFs are the same as that of bare MOF. Thus, these molecules do not affect MOF's stability. However, the hardness of NO and NO_2 is higher than that of bare MOF. Therefore, these molecules make the MOF more stable or less reactive. The value of softness yields similar outcomes. Similar results are obtained in the case of the M06 method, and the values of the descriptors are mentioned in Table S3 of supportive information.

As the value of the frontier orbital gap varies, so does the molecules' conductivity. Consequently, we may detect gas molecules via the MOF by employing the idea of the frontier orbital gap. In the B3LYP method, it is found that the frontier orbital gap of MOFs loaded with CO, H_2S, SO_2, and NH_3 is more or less identical to that of bare MOF. Therefore, these molecules are undetectable to Mg-MOF-74. However, the frontier orbital gap of MOFs loaded with NO and NO_2 is not comparable with that of bare MOFs. Based on this, Mg-MOF-74 can identify these molecules, and the results of the M06 method support this assertion completely.

https://doi.org/10.1021/acsomega.3c08358
ACS Omega 2024, 9, 4849−4856

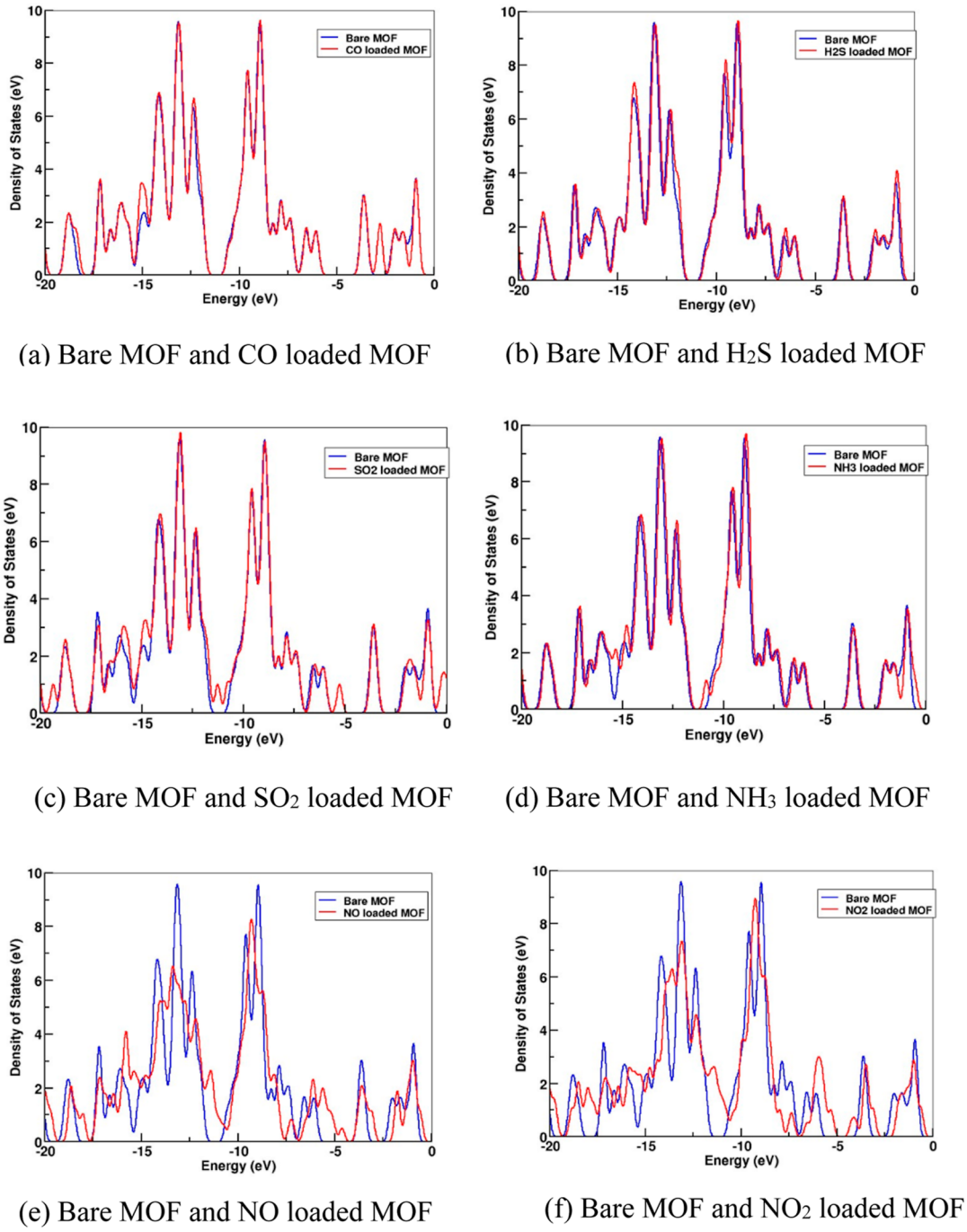

Figure 6. Comparison of the density of states of various loaded MOFs with bare MOFs using the B3LYP method.

Mulliken Charge Analysis. The simplest representation of the charge distribution is provided by the Mulliken population. The charge distributions over the atoms indicate that charge transfer in the molecule involves the production of donor and acceptor pairs. Because of how atomic charges affect dipole moments, molecular polarizability, electronic structure, and other features of molecular systems, it is crucial in the application of quantum chemical calculations to molecular systems.[26] In both B3LYP and M06 functionals at 6-31G* level theories, the Mulliken charge distribution of the bare and loaded MOFs is determined. Figure 5 shows the Mulliken charge distribution on bare and loaded MOFs obtained by the M06 method. The charge distribution is depicted by color coding based on the spectrum. On six different gas-loaded MOFs as well as bare MOFs, the charge distributions have been analyzed. The guest molecules and MOF are both electrically neutral before adsorption; however, it is found that all of the guest molecules get positively charged after adsorption (except the NO_2-loaded MOF in the B3LYP method), whereas the MOF turns negatively charged. This means that the guest molecules lose electrons while MOF gains electrons. The total charge on the guest molecules after adsorption is given in Table 3.

The binding energy calculation shows that the binding energies of CO and H_2S with MOF fall in the physisorption range, while those of SO_2, NH_3, NO, and NO_2 are in the chemisorption range. However, Mulliken charge analysis reveals that the molecules do not lose electrons according to

https://doi.org/10.1021/acsomega.3c08358
ACS Omega 2024, 9, 4849−4856

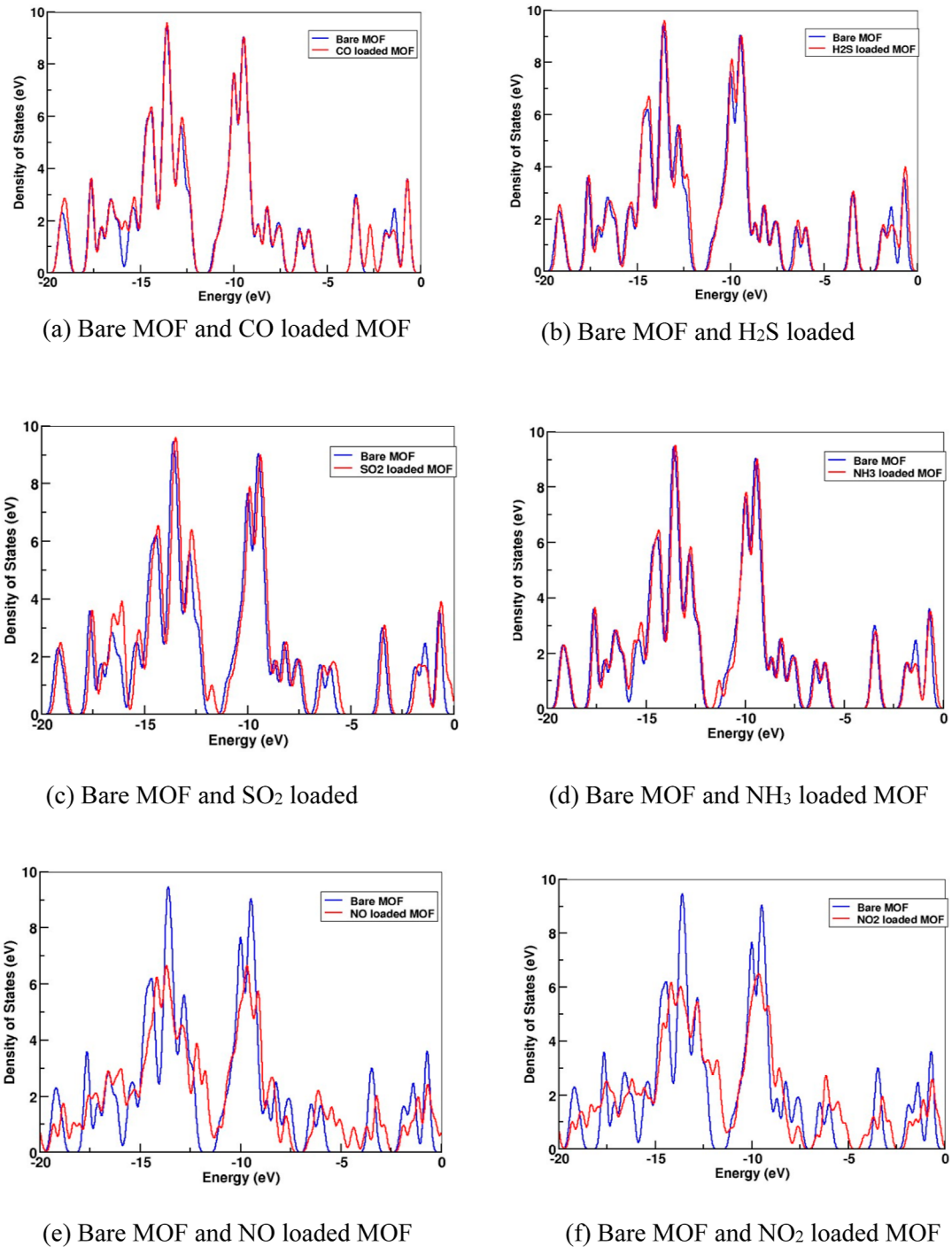

Figure 7. Comparison of the density of states of various loaded MOFs with bare MOFs using the M06 method.

the interaction energy. The higher interaction energy is typically indicated by greater charge transfer between two entities, but the connection between the interaction energy and charge transfer is not always straightforward; for instance, orbital overlap and the existence of additional functional groups can all be significant.

As the MOF gains electrons from the guest molecules, its density of states changes after the adsorption. The comparison of the density of states of bare MOF and loaded MOFs is shown in Figures 6 and 7. In comparison to other loaded MOFs, it is found that the density of states of NO and NO_2 loaded MOFs fluctuates significantly.

Molecular electrostatic potential. A molecular electrostatic potential (MEP) is a crucial tool for assessing and predicting the relative reactive sites for both electrophilic and nucleophilic attacks. MEP surfaces of different MOFs obtained by the M06 method are shown in Figure 8. The varying electrostatic potential values on the MEP surfaces give rise to their distinct colors. Blue is the highest potential value, followed by green, yellow, orange, and red. Both the B3LYP and M06 methods are used to analyze MEP surfaces at the 6-31G* level theories in order to identify the reactive regions for the MOF.

https://doi.org/10.1021/acsomega.3c08358
ACS Omega 2024, 9, 4849−4856

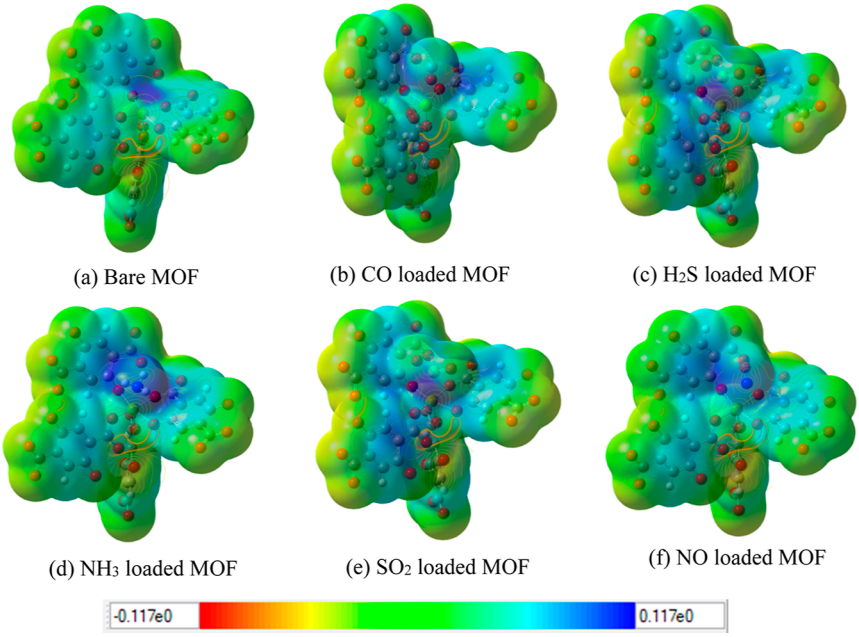

Figure 8. Electrostatic potential map of various MOFs using the M06 method.

In the figure, the MEP diagram of the bare MOF shows that electron deficiencies, or blue color, are concentrated around the node region, which is vulnerable to nucleophilic attack. However, as one approaches the frontier sites, electron availability increases, and the color changes to light blue, green, and finally yellow at the front sites. The yellow color shows the presence of a slightly negative potential, which makes it vulnerable to electrophilic attack. In the same way, the MEP diagrams of loaded MOFs show that the guest molecules enter and remain in the region of electron deficiencies (blue region), diluting and spreading the "blue" region outward from the node. Therefore, the guest molecules reduce the positive potential around the node and extend its regions toward the frontier sites.

CONCLUSIONS

Using a first-principles approach based on DFT, the structural and electronic properties of the Mg-MOF-74 crystal are investigated. It is found that the crystal is nonmagnetic and semiconducting by nature. The binding energies of six different toxic gas molecules with the MOFs are calculated. Among these molecules, the binding energies of CO and H_2S molecules are in the range of physisorption, whereas those of SO_2, NH_3, NO, and NO_2 molecules are in the range of chemisorption. The binding energies of NO and NO_2 are much greater than those of the other molecules, suggesting that these molecules are most stable in Mg-MOF-74. The binding energies of nitrogen-containing gas molecules are greater than those of other molecules. This is because the last unpaired electron of nitrogen may strongly interact with the mg^{+2} node of the MOF. The HOMO−LUMO gap of the MOF is changed after loading NO and NO_2, indicating that Mg-MOF-74 is a good detector for these gases. The value of the hardness/softness of the bare MOF is increased/decreased after the loading of NO and NO_2. Therefore, these gas molecules increase the stability of the MOF. However, due to their identical hardness/softness values to those of bare MOF, the CO, H_2S, SO_2, and NH_3 molecules do not affect the stability of MOF.

ASSOCIATED CONTENT

Supporting Information

The Supporting Information is available free of charge at https://pubs.acs.org/doi/10.1021/acsomega.3c08358.

Volume of the primitive cell, coordinates and absolute energies of the cluster, coordinates and absolute energies of loaded MOF/CO, molecular orbital distribution, chemical reactivity descriptors, and Mulliken charge analysis (PDF)

AUTHOR INFORMATION

Corresponding Author

Dipak Adhikari − *Central Department of Physics, Tribhuvan University, Kathmandu 44600, Nepal;* orcid.org/0009-0007-4270-462X; Email: adipak098@gmail.com

Authors

Ravi Karki − *Central Department of Physics, Tribhuvan University, Kathmandu 44600, Nepal*

Kapil Adhikari − *Gandaki University, Pokhara 33700, Nepal*

Nurapati Pantha − *Central Department of Physics, Tribhuvan University, Kathmandu 44600, Nepal*

Complete contact information is available at: https://pubs.acs.org/10.1021/acsomega.3c08358

Notes

The authors declare no competing financial interest.

ACKNOWLEDGMENTS

The authors would like to acknowledge Prof. Dr. N.P. Adhikari and Dr. Hari Paudel for valuable insights.

REFERENCES

(1) Adhikari, D.; Karki, R.; Adhikari, K.; Pantha, N. Adsorption of toxic gases by metal-organic frameworks. *HimPhys* **2023**, *10*, 1−24.

(2) Bobbitt, N. S.; Mendonca, M. L.; Howarth, A. J.; Islamoglu, T.; Hupp, J. T.; Farha, O. K.; Snurr, R. Q. Metal-organic frameworks for the removal of toxic industrial chemicals and chemical warfare agents. *Chem. Soc. Rev.* **2017**, *46* (11), 3357−3385.
(3) Islamoglu, T.; Chen, Z.; Wasson, M. C.; Buru, C. T.; Kirlikovali, K. O.; Afrin, U.; Mian, M. R.; Farha, O. K. Metal-organic frameworks against toxic chemicals. *Chem. Rev.* **2020**, *120* (16), 8130−8160.
(4) Zhou, X.; Su, Z.; Chen, H.; Xiao, X.; Qin, Y.; Yang, L.; Yan, Z.; Sun, W. Capture of pure toxic gases through porous materials from molecular simulations. *Mol. Phys.* **2018**, *116* (15−16), 2095−2107.
(5) Khan, N. A.; Hasan, Z.; Jhung, S. H. Adsorptive removal of hazardous materials using metal-organic frameworks (mofs): A review. *J. Hazard. Mater.* **2013**, *244*−*245*, 444−456.
(6) Li, J.-R.; Kuppler, R. J.; Zhou, H.-C. Selective gas adsorption and separation in metal-organic frameworks. *Chem. Soc. Rev.* **2009**, *38* (5), 1477−1504.
(7) Jiang, C.; Wang, X.; Ouyang, Y.; Lu, K.; Jiang, W.; Xu, H.; Wei, X.; Wang, Z.; Dai, F.; Sun, D. Recent advances in metal-organic frameworks for gas adsorption/separation. *Nanoscale Adv.* **2022**, *4* (9), 2077−2089.
(8) Farrusseng, D.; Aguado, S.; Pinel, C. Metal-organic frameworks: opportunities for catalysis. *Angew. Chem., Int. Ed.* **2009**, *48* (41), 7502−7513.
(9) Kumar, P.; Deep, A.; Kim, K.-H. Metal-organic frameworks for sensing applications. *TrAC, Trends Anal. Chem.* **2015**, *73*, 39−53.
(10) Karki, R.; Adhikari, D.; Adhikari, K.; Pantha, N. Metal-organic frameworks (mofs) as efficient carrier for targeted nanodrug delivery. *HimPhys* **2020**, *9*, 1−10.
(11) Furukawa, H.; Ko, N.; Go, Y. B.; Aratani, N.; Choi, S. B.; Choi, E.; Yazaydin, A. O.; Snurr, R. Q.; O'Keeffe, M.; Kim, J.; et al. Ultra-high porosity in metal-organic frameworks. *Science* **2010**, *329* (5990), 424−428.
(12) Soni, S.; Bajpai, P. K.; Arora, C. A review on metal-organic framework: Synthesis, properties and application. *Charact. Appl. Nanomater.* **2020**, 3 (2), 87−106.
(13) Alonso, G.; Bahamon, D.; Keshavarz, F.; Giménez, X.; Gamallo, P.; Sayos, R. Density functional theory-based adsorption isotherms for pure and flue gas mixtures on mg-mof-74. application in co2 capture swing adsorption processes. *J. Phys. Chem. C* **2018**, *122* (7), 3945−3957.
(14) Giannozzi, P.; Baroni, S.; Bonini, N.; Calandra, M.; Car, R.; Cavazzoni, C.; Ceresoli, D.; Chiarotti, G. L.; Cococcioni, M.; Dabo, I.; et al. Quantum espresso: a modular and open-source software project for quantum simulations of materials. *J. Phys.: Condens. Matter* **2009**, *21* (39), 395502.
(15) Frisch, M.; Trucks, G.; Schlegel, H.; Scuseria, G.; Robb, M.; Cheeseman, J.; Scalmani, G.; Barone, V.; Mennucci, B.; Petersson, G.; et al. *Gaussian 09*. revision d. 01; gaussian, inc.: wallingford ct, 2009. See also: URL:. http://www.gaussian.com.
(16) Becke, A. D. Density-functional thermochemistry. i. the effect of the exchange-only gradient correction. *J. Chem. Phys.* **1992**, *96* (3), 2155−2160.
(17) Stephens, P. J.; Devlin, F. J.; Chabalowski, C. F.; Frisch, M. J. Ab initio calculation of vibrational absorption and circular dichroism spectra using density functional force fields. *J. Phys. Chem.* **1994**, *98* (45), 11623−11627.
(18) Lee, C.; Yang, W.; Parr, R. Development of the Colle-Salvetti correlation-energy formula into a functional of the electron density. *Phys. Rev. B* **1988**, *37*, 785−789.
(19) Zhao, Y.; Truhlar, D. G. The m06 suite of density functionals for main group thermochemistry, thermochemical kinetics, noncovalent interactions, excited states, and transition elements: two new functionals and systematic testing of four m06-class functionals and 12 other functionals. *Theor. Chem. Acc.* **2008**, *120*, 215−241.
(20) Rassolov, V. A.; Pople, J. A.; Ratner, M. A.; Windus, T. L. 6-31g* basis set for atoms k through zn. *J. Chem. Phys.* **1998**, *109* (4), 1223−1229.
(21) Rassolov, V. A.; Ratner, M. A.; Pople, J. A.; Redfern, P. C.; Curtiss, L. A. 6-31g* basis set for third-row atoms. *J. Comput. Chem.* **2001**, *22* (9), 976−984.
(22) Rosen, A. S.; Notestein, J. M.; Snurr, R. Q. Comparing gga, gga + u, and meta-gga functionals for redox-dependent binding at open metal sites in metal-organic frameworks. *J. Chem. Phys.* **2020**, *152* (22), 224101.
(23) de Oliveira, A.; de Lima, G. F.; De Abreu, H. A. Structural and electronic properties of m-mof-74 (m= mg, co or mn). *Chem. Phys. Lett.* **2018**, *691*, 283−290.
(24) Lian, L.; Guo, L.; Guo, C. Adsorption of Congo red from aqueous solutions onto Ca-bentonite. *J. Hazard. Mater.* **2009**, *161* (1), 126−131.
(25) Valenzano, L.; Civalleri, B.; Chavan, S.; Palomino, G. T.; Areán, C. O.; Bordiga, S. Computational and experimental studies on the adsorption of co, n2, and co2 on mg-mof-74. *J. Phys. Chem. C* **2010**, *114* (25), 11185−11191.
(26) Sangeetha, V.; Govindarajan, M.; Kanagathara, N.; Marchewka, M.; Drozd, M.; Anbalagan, G. Vibrational, dft, and thermal analysis of 2, 4, 6-triamino-1, 3, 5-triazin1-ium 3-(prop-2-enoyloxy) propanoate acrylic acid monosolvate monohydrate. *J. Mol. Struct.* **2013**, *1054*−*1055*, 307−320.

https://doi.org/10.1021/acsomega.3c08358
ACS Omega 2024, 9, 4849−4856